Supplemental Information

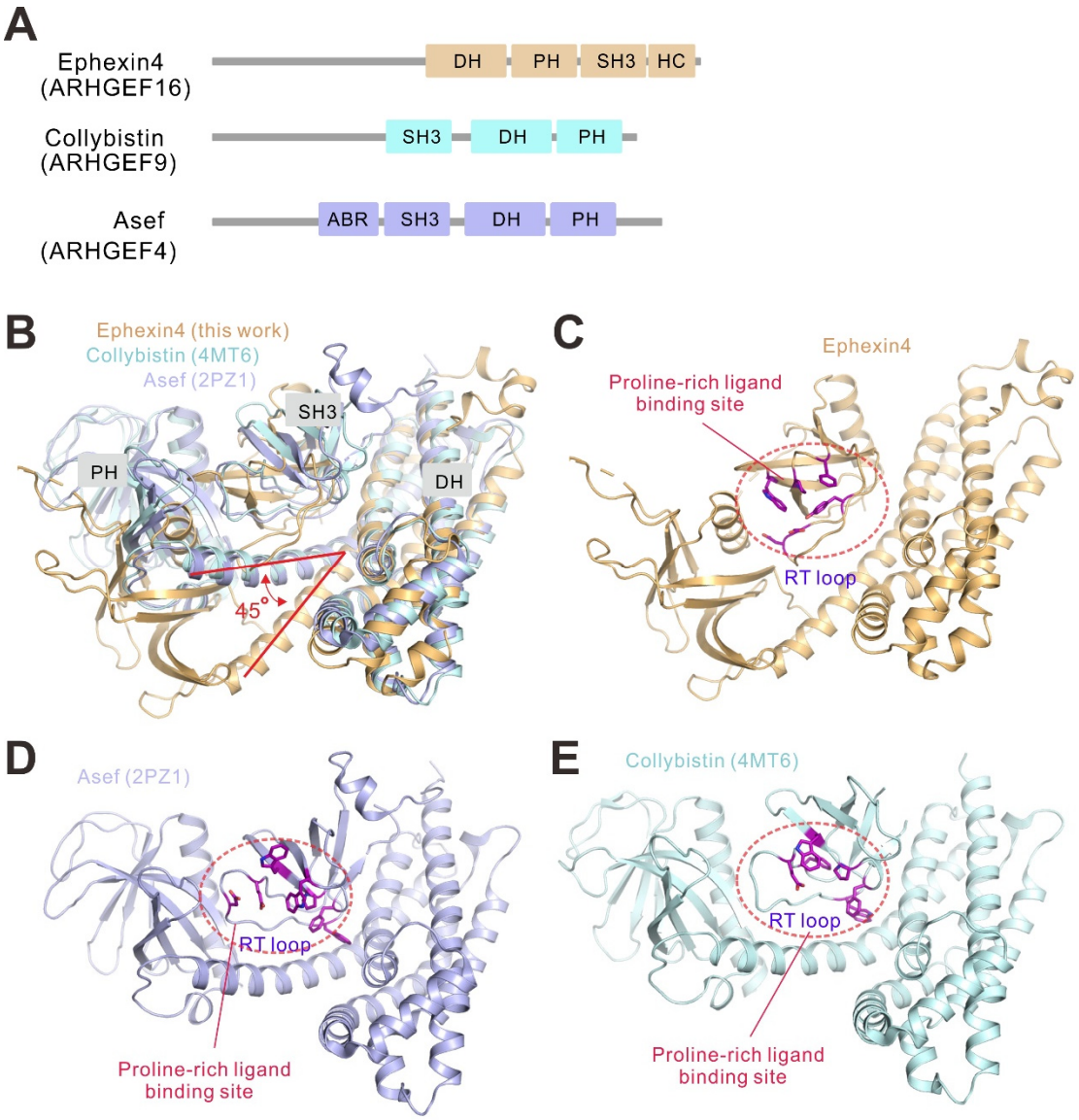

Fig. S1. Structural comparison between Ephexin4, Collybistin, and Asef. (A) Domain organizations of Ephexin4, Collybistin, and Asef. **(B)** Superimposition of Ephexin4 DH-PH-SH3 structure with Collybistin SH3-DH-PH structure (PDB code: 4MT6), and Asef SH3-DH-PH structure (PDB code: 2PZ1). **(C-E)** Ribbon diagram representations of the structures of Ephexin4 **(C)**, Asef **(D)**, and Collybistin **(E)**. The canonical proline-rich ligand binding site (RT-loop) on the SH3 domain of the three proteins are indicated with red circles.

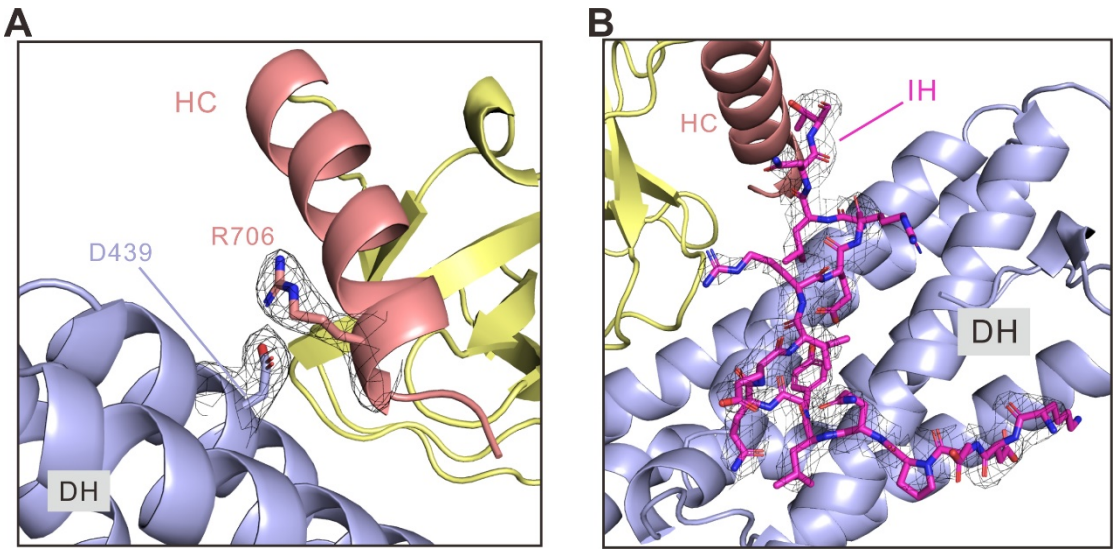

Fig. S2. The electron density map of DH-HC and DH-IH interface. (A) Electron density map for the interface of DH−HC. The sidechains of R706 and D439 are shown in sticks. **(B)** Electron density map for the IH region. Residues in the IH region are shown in sticks. The 2Fo-Fc electron density maps are colored in grey, and contoured at 1.0 σ.

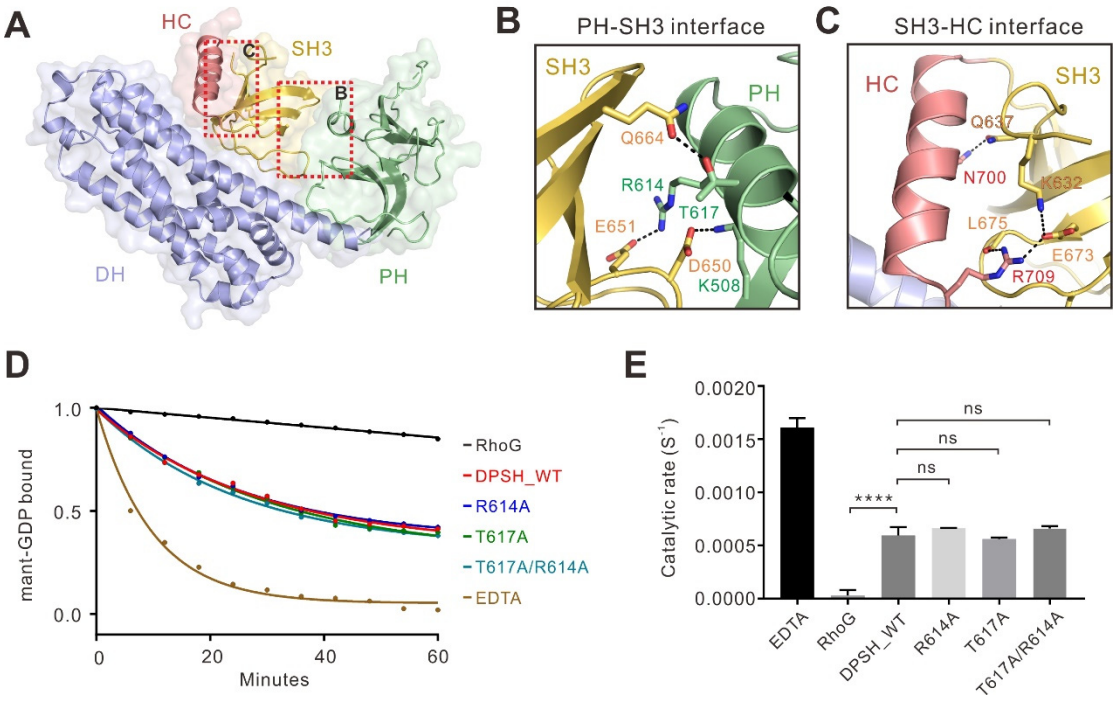

Fig. S3. The PH-SH3 interface plays a less important role in repression of GEF activity. (A) The combined surface and ribbon representations of the Ephexin4^{DPSH} structure. **(B-C)** Zoomed-in view of the PH−SH3 **(B)** and SH3−HC **(C)** interface. **(D)** *In vitro* GEF assays showing that the residues in PH−SH3 interface are not crucial for inhibition of GEF activity. All GEF experiments were performed using three independent protein preparations with at least duplicate measurements. The data shown was from one representative experiment. **(E)** Quantification of GEF experiments testing the role of residues at PH−SH3 interface in regulation of Ephexin4 activity. Values are expressed as mean ± SD. ns, not significant, ****p < 0.0001.

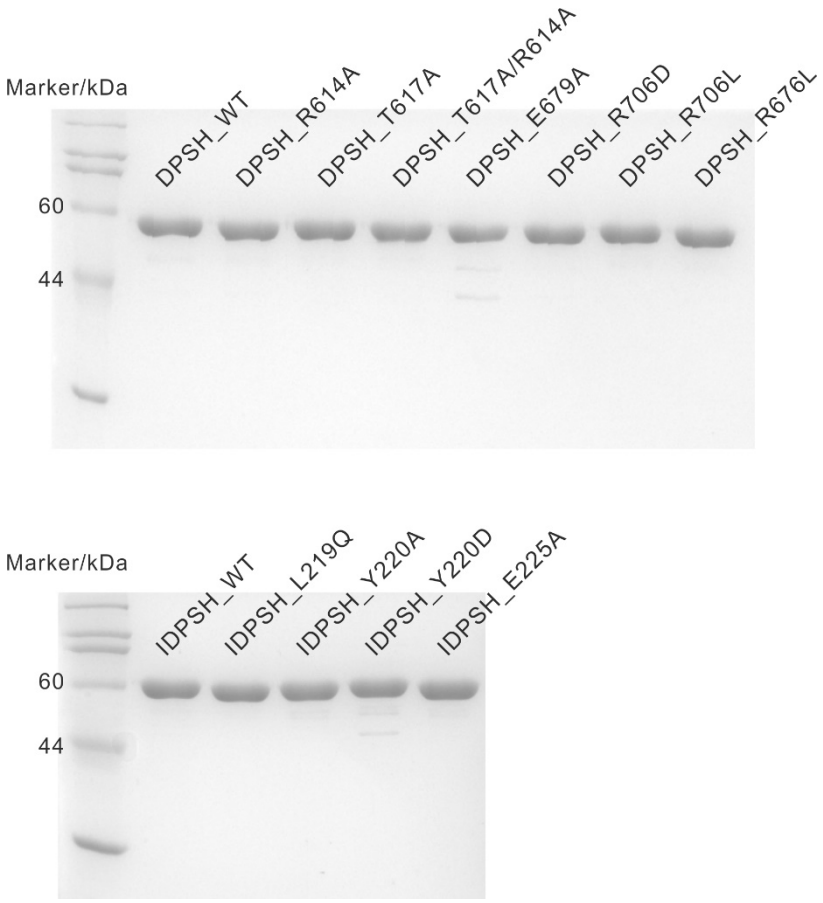

Fig. S4. SDS-PAGE analysis of freshly purified wild type and mutant forms of DPSH and IDPSH proteins used in GEF assays.

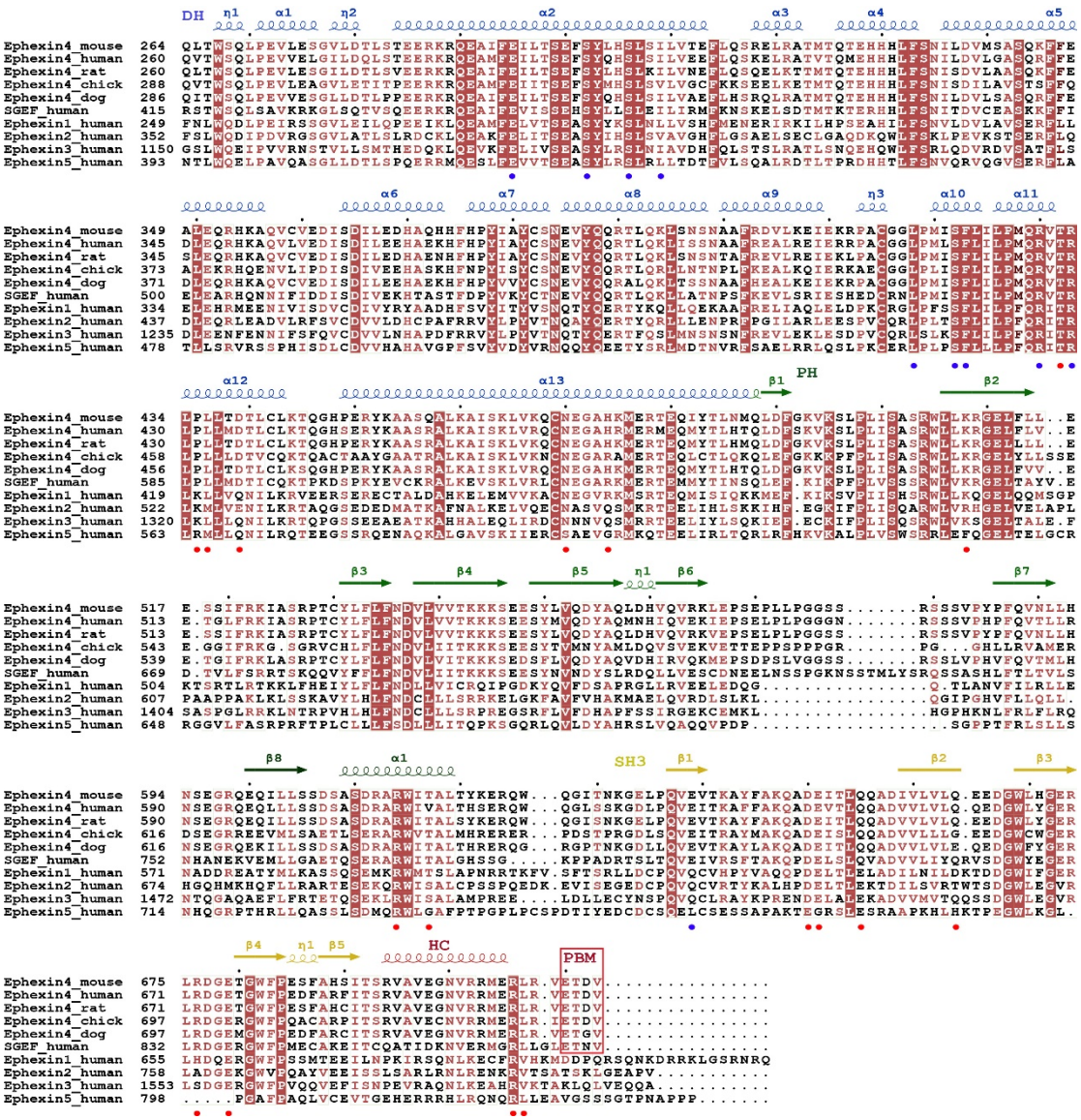

Fig. S5. Structure-based sequence analysis of Ephexin family proteins and SGEF. In this alignment, the identical residues are highlighted with red boxes, and the conserved residues are color in red. Residues required for C-terminal inhibition and N-terminal inhibition are indicated by red and blue dots, respectively.

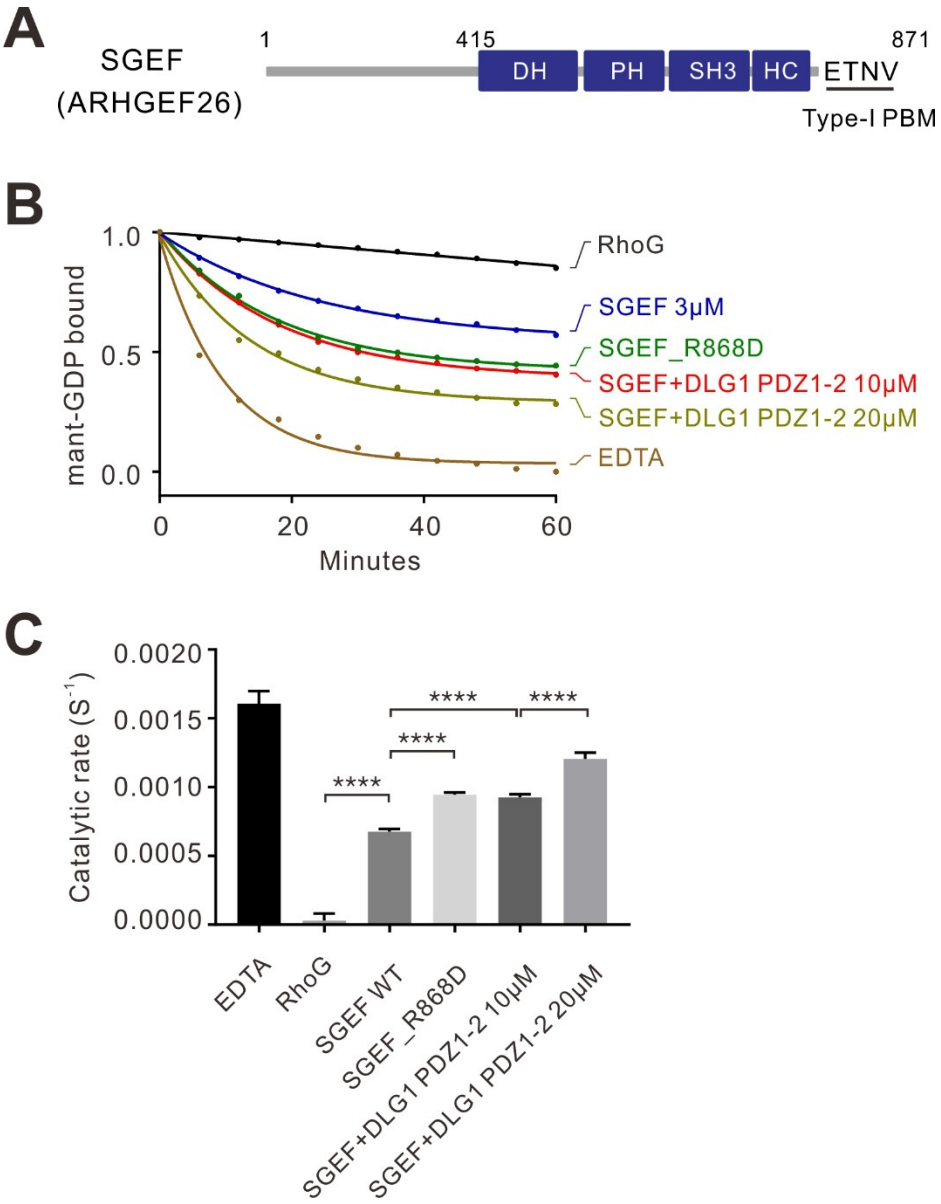

Fig. S6. Binding of DLG1 activates autoinhibited SGEF. (**A**) Domain organization of SGEF. Noted that the type-I PDZ-binding motif (PBM) (sequence:- ETNV) is also shown. **(B)** *In vitro* GEF assays showing that substitution of R868 (the corresponding residue in Ephexin4 is R706 which involves in HC-DH interaction) with Asp significantly increased its GEF activity. Also, binding of DLG1 PDZ1-2 led to an increased GEF activity toward RhoG. In this experiment, the concentration of SGEF (SGEF_R868D) and RhoG are 3 μM and 2 μM, respectively. All GEF assays were performed using three independent protein preparations with at least duplicate measurements. The data shown was from one representative experiment. **(C)** Quantification of GEF experiments testing the role of the DLG1 PDZ domains in regulation of SGEF activity. All results are expressed as mean ± SD. ****$p < 0.0001$.

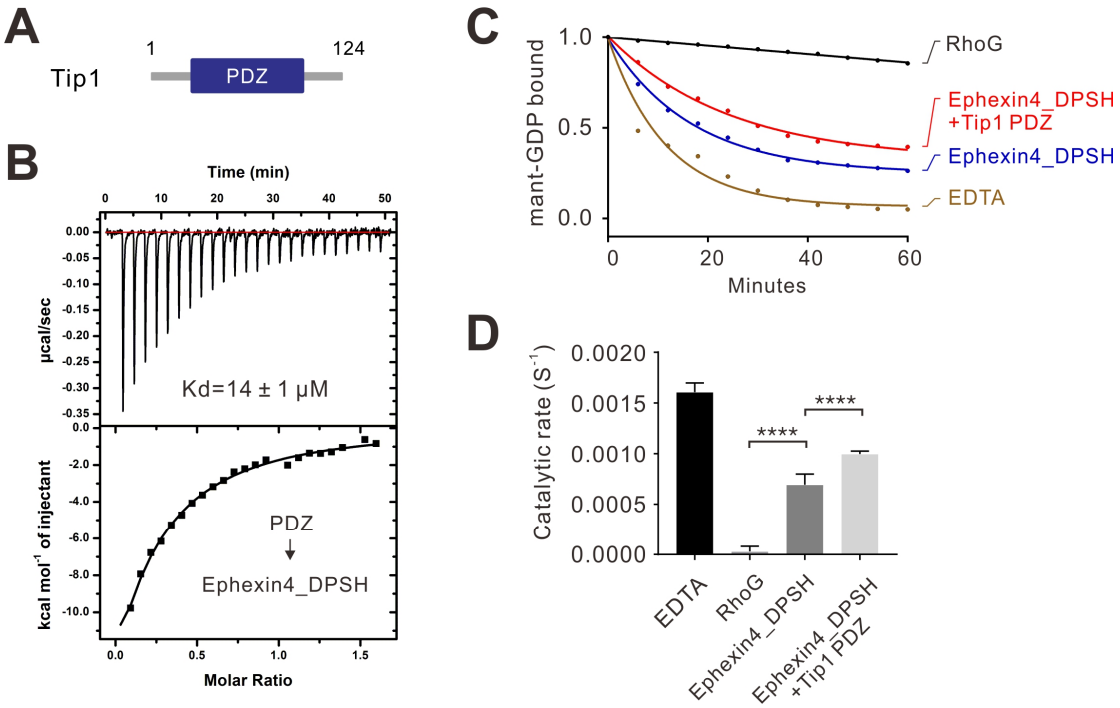

Fig. S7. Binding of Tip1 activates autoinhibited Ephexin4. (**A**) Domain organization of Tip1. (**B**) ITC-based measurement of the binding affinity between Tip1 PDZ and Ephexin4^{DPSH}. **(C)** *In vitro* GEF assays showing that binding of Tip1 PDZ1 led to an increased GEF activity of Ephexin4^{DPSH} toward RhoG. All GEF experiments were performed using three independent protein preparations with at least duplicate measurements. The data shown was from one representative experiment. **(D)** Quantification of GEF experiments testing the role of the Tip PDZ1 domain in regulation of Ephexin4 activity. All results were expressed as mean ± SD. ****p < 0.0001.

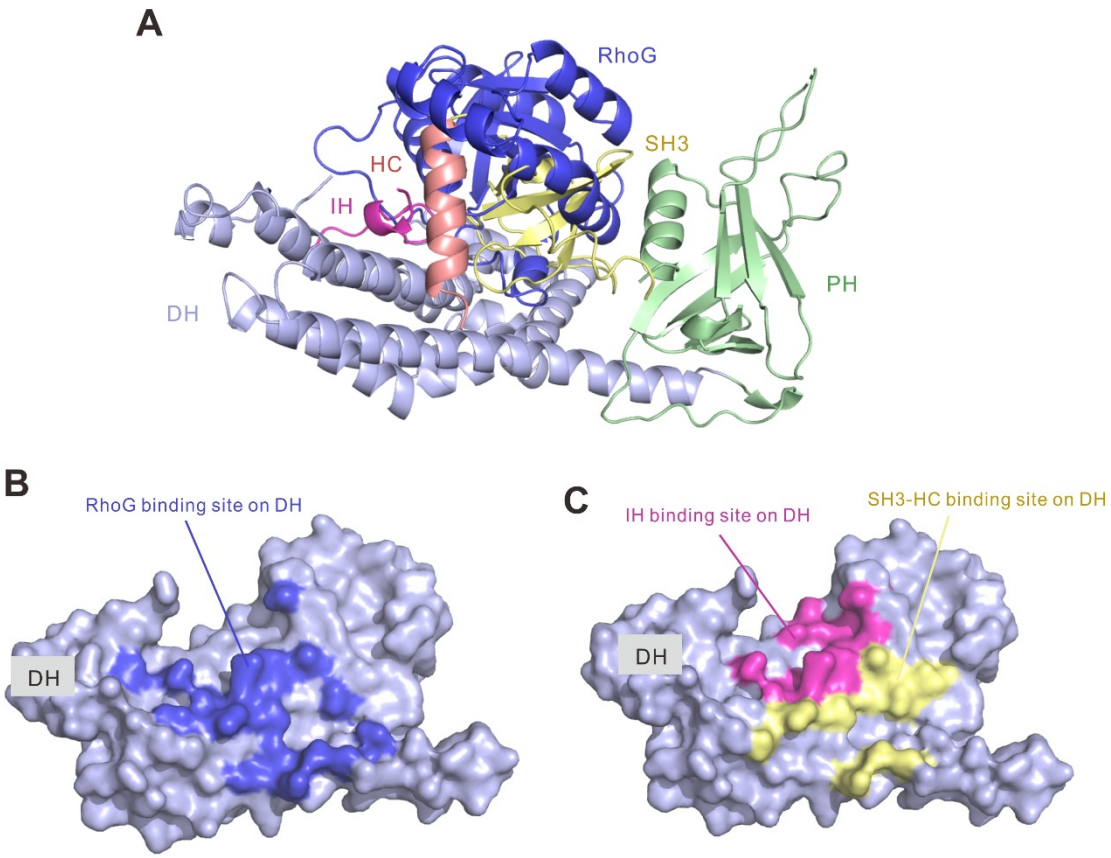

Fig. S8. Structural analysis of the binding site of RhoG and inhibitory elements on DH domain of Ephexin4. (A) Superposition of RhoG−DH modeled complex structure and IDPSH structure (this study). **(B-C)** Surface diagram of binding site of RhoG **(B)** and inhibitory elements **(C)** on DH domain. The GEF-bound structure of RhoG was modelled by Swiss-model (https://swissmodel.expasy.org), using RhoA structure (PDB: 1XCG) as the template. Docking of RhoG−Ephexin4 DH−PH complex structure was performed by ZDOCK server (http://zdock.umassmed.edu).

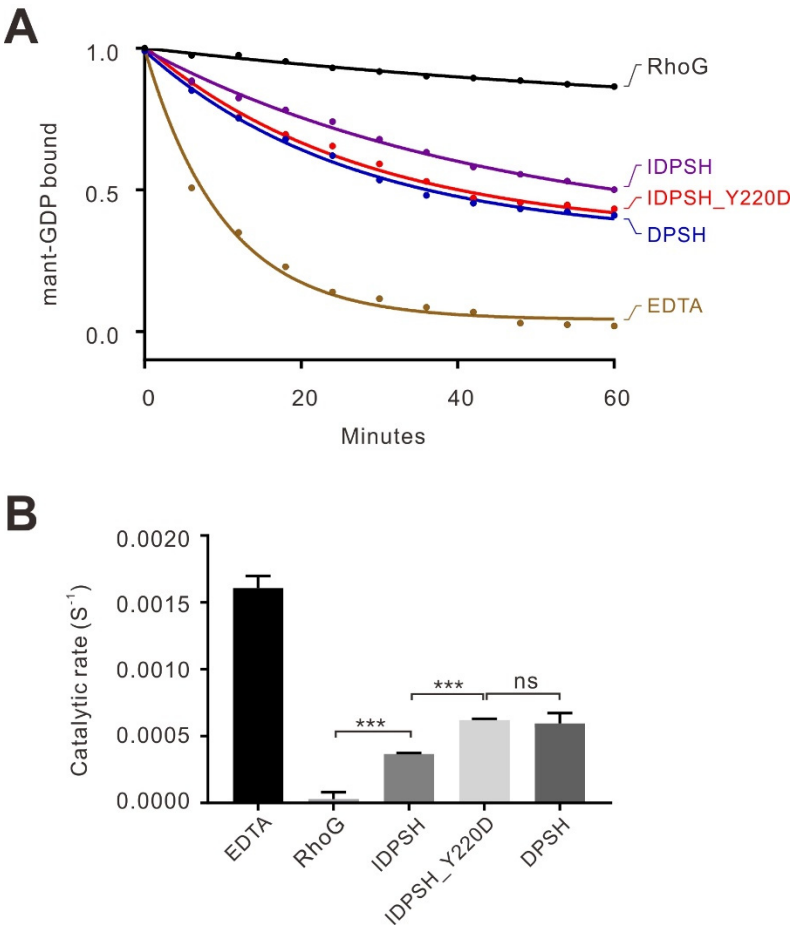

Fig. S9. Comparison of GEF activity between IDPSH, IDPSH_Y220D, and DPSH. **(A)** *In vitro* GEF assays showing that IDPSH_Y220D displayed a similar GEF activity as DPSH. All GEF assays were performed using three independent protein preparations with at least duplicate measurements. The data shown was from one representative experiment. **(B)** Quantification of GEF experiments using various forms of Ephexin4 shown in **(A)**. All results were expressed as mean ± SD. ns, not significant; ***p < 0.001.

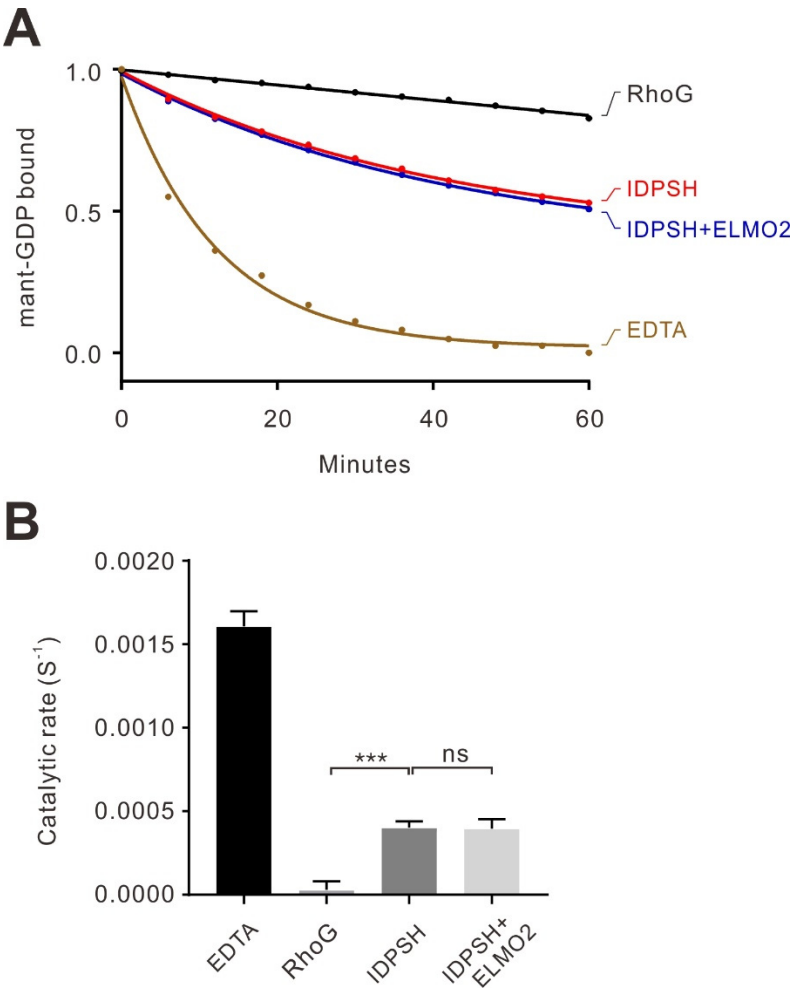

Fig. S10. Full length ELMO2 did not activate Ephexin4^{IDPSH}. (A) *In vitro* GEF assays of Ephexin4^{IDPSH} with or without ELMO2. All GEF assays were performed using three independent protein preparations with at least duplicate measurements. The data shown was from one representative experiment. **(B)** Quantification of GEF experiments testing the role of ELMO2 in regulation of Ephexin4 activity shown in **(A)**. All results were expressed as mean ± SD. ns, not significant; ***$p < 0.001$.